INVESTIGATION OF LUNAR SPINELS AT SINUS AESTUUM. C. M. Weitz[1], M. I. Staid[1], L. R. Gaddis[2], S. Besse[3], and J. M. Sunshine[4], [1]Planetary Science Institute, 1700 E Fort Lowell, Suite 106, Tucson, AZ 85719 (weitz@psi.edu), [2]Astrogeology Science Center, U. S. Geological Survey, 2255 N. Gemini Drive, Flagstaff, AZ 86001; [3]Camino Bajo del Castillo s/n, Ur. Villafranca del Castillo, 28692 Villanueva de la Canada, Madrid, Spain; [4]Dept of Astronomy, University of Maryland, College Park, MD.

Introduction: Recent remote sensing observations by the Moon Mineralogy Mapper (M^3) on the Chandrayaan-1 spacecraft and the Spectral Profiler (SP) on the SELENE Kaguya orbiter have identified spinels in numerous locations across the Moon [1-3]. The Mg-rich spinels have a prominent 2 µm absorption and lack any 1 µm absorption, which allows them to be identified and distinguished from other lunar materials. SP data analyzed by [3] was used to identify a visible-wavelength absorption feature around 0.7 µm along with a strong 2 µm absorption only at Sinus Aestuum (SA). They attributed the 0.7 µm feature to the presence of a Fe- or Cr-bearing spinel rather than the Mg-spinel more commonly identified on the Moon [2]. The Fe- or Cr-rich spinels in the SA region are associated with widespread, dark pyroclastic deposits [1,3,4].

In this study, we analyzed M^3 data for spinel locations at SA, and then examined visible images from the Lunar Reconnaissance Orbiter (LRO) Narrow Angle Camera (NAC) and Wide Angle Camera (WAC), as well as the Kaguya Terrain Camera (TC) and Multiband Imager (MI) images to correlate these spinel signatures to surface morphologic features. We extracted M^3 spectra of several spinel locations and attempted to understand what was creating the signatures throughout SA. Finally, we examined the locations where SP data showed visible-wavelength features in the spinel spectra and compared them to locations where M^3 data showed a 0.7 µm feature.

Observations: We identified the strongest and largest spinel signatures in widespread sites across the highlands and some mare of Sinus Aestuum (Fig. 1, where green circles indicate that a 0.7 µm absorption is present and blue circles mark sites with a weak or no 0.7 µm signature). We then examined WAC, NAC, and Kaguya TC visible images for these spinel locations. In all cases, we identified an impact crater in association with the spinel signature (Fig. 2). The crater diameters ranged from ~100 m to ~4 km, which corresponds to transient crater excavation depths of ~25-1000 m [5,6], although for the larger craters (i.e., >1 km diam.) the spinels were observed along the upper crater walls rather than in the ejecta, suggesting shallower depths for the spinels. The majority of spinel deposits are associated with DMD on the highlands. Nine of the circles correspond to small impact craters with spinel deposits that are on the highlands but not associated with any obvious surface exposures of DMD. The remaining spinels are found in association with craters on the mare.

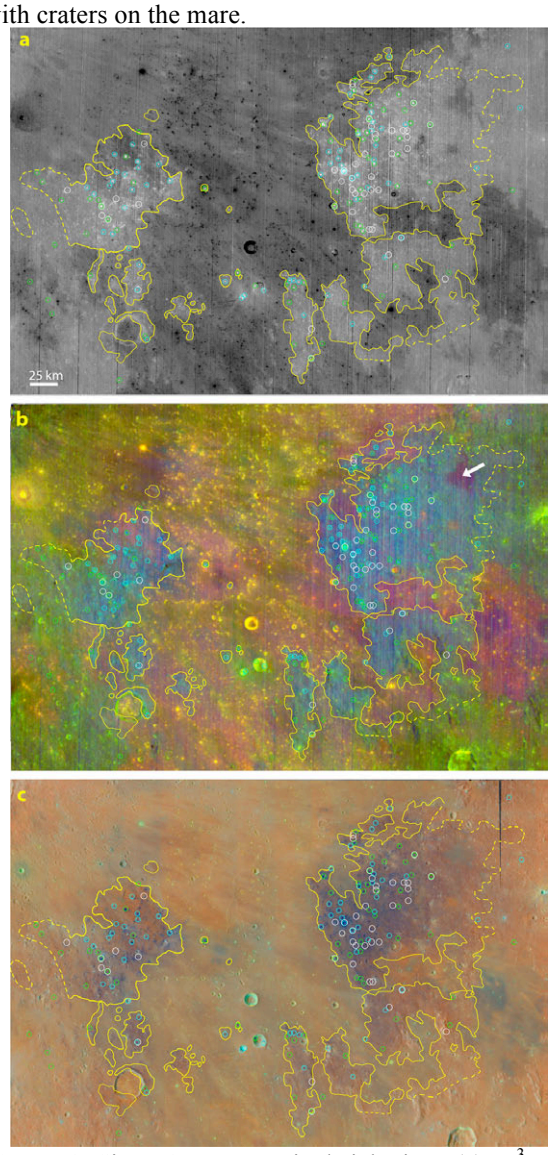

Figure 1. Sinus Aestuum spinel-rich sites. (a) M^3 mosaic showing the 2 µm integrated band depth (IBD) ratioed to the 1 µm IBD. The areal extent of the DMD on the highlands is noted by the yellow line. White circles represent locations where [3] identified spinels with visible-wavelength signatures in Kaguya SP data. (b) Color M^3 mosaic (R=1 µm IBD, G=2 µm IBD, B=700 nm IBD). White arrow identifies a mare pond in the SA highlands. (c) Color ratio MI MAP mosaic (R=750/415 nm, G=750/950 nm, B=415/750 nm) merged with WAC basemap mosaic.

The main morphologic difference between those craters that exhibit the strong 0.7 µm absorption and those that do not appears to be in the freshness of the crater appearance, although there are exceptions. Our observations are consistent with a spinel deposit of variable thickness and a widespread, heterogeneous distribution, with likely variable ratios of mixtures of spinel and DMD within the highlands regolith.

We identified several larger (>1 km diameter) highland impact craters that exhibit spinel signatures along the interior crater rim but not in the ejecta. The spinel is best identified in fresh exposures of the regolith, such as along the crater interior walls where mass wasting on the steeper slopes exposes immature regolith containing the spinels. For all these craters, there is no obvious source layer for the spinel observed along the crater walls.

We identified nine larger spots in Figure 1 where we found a spinel signature in the highlands but outside of the mapped DMD. Examination of NAC and TC images for these nine locations showed a small (100-400 m diameter) impact crater associated with the spinel signature. The remaining spinel spots are associated with four larger (3.5-11 km diameter) impact craters (Gambart B, Gambart G, Gambart L, and Schroter D) and one smaller crater (350 m diameter) in the mare. All four larger craters have low reflectance debris along portions of their interior walls that corresponds to the spinel signatures. The dark spinel-bearing materials are observed starting near the top of the walls and spread down to the crater floors. There is no obvious layer or bedrock within the crater wall that appears to be the source for the spinel. Spectra taken from the crater surroundings show remnant highland materials are present within the mare, and it appears that the spinel signatures actually occur in highland materials rather than in the mare.

We also examined all thirty-seven spots from [3] in our M^3 data. Most of the SP sites are only 1-2 SP pixels across, which equates to <100 m in size. A search for these small SP sites in M^3 data did reveal possible corresponding spinel detections within the latitude and longitude range listed in Table S1 of [3]. In contrast, SP data did not find all the M^3 detections of spinels with 0.7 µm features.

Discussion: Our new M^3 results indicate that Fe- or Cr-spinels with 0.7 µm absorptions are mixed into most of the DMD across the Sinus Aestuum highlands. The discrepancy between spinel detections made by SP and M^3 is simply a function of the more limited spatial distribution of the SP data compared to M^3 data across the SA region. Consequently, our M^3 analysis provides a more comprehensive understanding of the spinel distribution at SA. The M^3 spectra extracted from spinel-rich locations show a visible-wavelength absorption, consistent with the SP results, although the location and width of the visible signature varies. Not all spinel spectra exhibit a strong visible-wavelength absorption, especially those spectra taken from slightly older craters.

The spinel deposits are strongly correlated to the distribution of pyroclastic deposits, indicating the two materials were most likely emplaced together as part of an explosive volcanic eruption. The spinels may have formed in the same magma chamber that produced the pyroclastic beads, or the spinels may reside in a pluton at depth that was assimilated into the magma as it made its way to the surface.

Although the spinels and pyroclastics may have once existed as a homogeneous deposit on the highlands, mixing by craters and regolith development over billions of years has created a heterogeneous distribution of both spinels and pyroclastics within the highlands of SA, and buried the deposit beneath younger lava flows on the mare. All the strongest visible-wavelength features in M^3 data correspond to the freshest-looking craters, although there are examples of young fresh craters in the highlands that do not display a spinel signature, consistent with a heterogeneous distribution of spinels within the highland soils.

References: [1] Sunshine J. M. et al. (2010) *LPSC 41*, Abstract #1508; [2] Pieters C. M. et al. (2011) *JGR 116*, 1-14. [3] Yamamoto S. et al. (2013) *Geophy. Res. Letts. 40*, 4549-4554. [4] Sunshine J.M. et al. (2014) LPSC 45, Abstract #2297. [5] Melosh J. (1989) *Impact Cratering, A Geologic Process*, Oxford Univ. Press. [6] Gaither T.A. et al. (2014) *LPSC 45*, Abstract 1933.

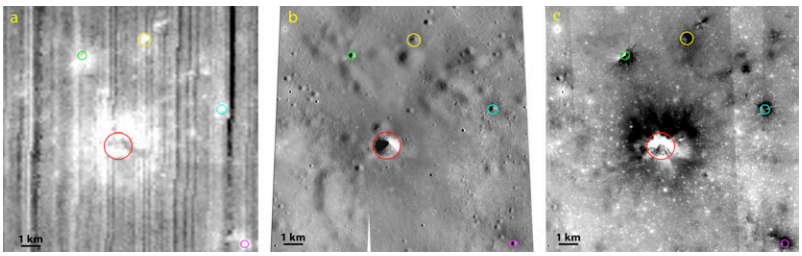

Fig. 2. Colored circles identify craters that have strong spinel signatures. (a) M^3 2 µm IBD divided by the 1 µm IBD ratio image. (b) NAC mosaic with images taken at high incidence angles and (c) small incidence angles.